In situ measurements of the spectral reflectance of metallic mirrors at the H_α line in a low density Ar–H plasma

Sven Dickheuer, Oleksandr Marchuk, Christian Brandt, Albrecht Pospieszczyk, Andrei Goriaev, Mykola Ialovega, Beatrix Göths, Yuri Krasikov, Andreas Krimmer, Philippe Mertens, and Arkadi Kreter

Citation: Review of Scientific Instruments **89**, 063112 (2018); doi: 10.1063/1.5024995

View online: https://doi.org/10.1063/1.5024995

View Table of Contents: http://aip.scitation.org/toc/rsi/89/6

Published by the American Institute of Physics

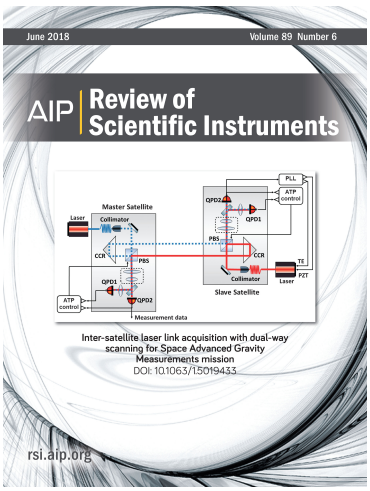

In situ measurements of the spectral reflectance of metallic mirrors at the H_α line in a low density Ar–H plasma

Sven Dickheuer,[1,a)] Oleksandr Marchuk,[1] Christian Brandt,[2] Albrecht Pospieszczyk,[1] Andrei Goriaev,[1] Mykola Ialovega,[1] Beatrix Göths,[1] Yuri Krasikov,[1] Andreas Krimmer,[1] Philippe Mertens,[1] and Arkadi Kreter[1]

[1]*Forschungszentrum Jülich GmbH, Institut für Energie- und Klimaforschung–Plasmaphysik, Partner of the Triliteral Euregio Cluster (TEC), 52425 Jülich, Germany*

[2]*Max-Planck-Institut für Plasmaphysik, 17491 Greifswald, Germany*

(Received 6 February 2018; accepted 23 May 2018; published online 13 June 2018)

The efficient and reliable control and monitoring of the quality of the optical properties of mirrors is an open problem in laboratory plasmas. Until now, the measurement of the reflectance of the first mirrors was based on the methods that require additional light calibration sources. We propose a new technique based on the ratio of the red- and blue-shifted emission signals of the reflected hydrogen atoms which enables the *in situ* measurement of the spectral reflectance of metallic mirrors in low-density Ar–H or Ar–D plasmas. The spectral reflectance coefficients were measured for C, Al, Ag, Fe, Pd, Ti, Sn, Rh, Mo, and W mirrors installed in the linear magnetized plasma device PSI-2 operating in the pressure range of 0.01-0.1 Pa. The results are obtained for the H_α line using the emission of fast atoms induced by excitation of H atoms through Ar at a plasma-solid interface by applying a negative potential $U = -80, \ldots, -220$ V to the mirror. The agreement between the measured and theoretical data of reflectance is found to be within 10% for the investigated materials (except for C). The spectra also allow us to efficiently determine the material of the mirror. https://doi.org/10.1063/1.5024995

I. INTRODUCTION

The accuracy and reliability of spectroscopic measurements in laboratory plasmas crucially depend on the physical properties of the optical components used. Usually, the accurate modeling and measurements of transmission, reflectance, polarization properties, etc., have to be performed well in advance of many experiments. For example, if an absolute intensity of a certain spectral line is measured, the transmittance of the complete optical path must be known. Here, the essential elements are the plasma facing mirrors that guide the emission from the plasma to the spectrometers or cameras. Mostly being placed inside the vacuum vessel, these mirrors may be damaged by exposure to the plasma (e.g., erosion and deposition) as for instance in fusion plasmas[1] or due to irritation induced by laser pulses.[2] The degradation of mirrors reduces the actual transmittance of the optical path so that a new calibration is required. Two practical solutions for this problem exist. In the most frequently applied method, a calibration lamp must be installed in front of the mirror to re-measure the reflectance. Either the calibration source must be placed inside the plasma volume or the mirror must be taken out. In the second and less frequently used approach, the measurements of the spectral reflectance can be monitored using another external source such as a laser.[3] However, this technique is often limited by the additional optical access to the mirror. Until now, no better practical method is known allowing for *in situ* measurements of the reflectance of plasma facing mirrors without removing it from the plasma and without using an additional calibration source. A more practical diagnostic to monitor the modification of surfaces, such as spectral reflectance, surface morphology, or polarization properties, is desired for fusion,[4] laser produced, or technological plasmas.[5,6]

A new method for measuring the spectral reflectance of electrical conductive surfaces such as metallic mirrors is proposed in this paper. It relies on the stimulated Balmer lines' emission in an Ar–H mixed plasma induced by fast hydrogen atoms. No additional calibration source is required, and there is no need to remove the mirror from the plasma. The calibration source is the plasma itself, and the fast atoms are generated as a result of the controlled plasma-surface interaction. The paper is structured as follows: In Sec. II, the background of the new diagnostic technique will be explained in detail. In Sec. III, we present the experimental results achieved by using the new diagnostic technique. The conclusion and outlook is given in Sec. IV.

II. DOPPLER-SHIFTED REFLECTANCE MEASUREMENT

The idea of this approach is sketched in Fig. 1. We consider the Doppler effect in front of a mirror. If an atom with velocity v moves toward the observer [Fig. 1(a), top], then the measured emission of the spectral lines is blue-shifted relative to the emission induced by an atom at rest according to the Doppler effect, i.e., $\Delta\lambda/\lambda_0 = (\lambda_b - \lambda_0)/\lambda_0 = v/c$, where λ_0 is the unshifted wavelength of the transition, λ_b is the measured

a)s.dickheuer@fz-juelich.de

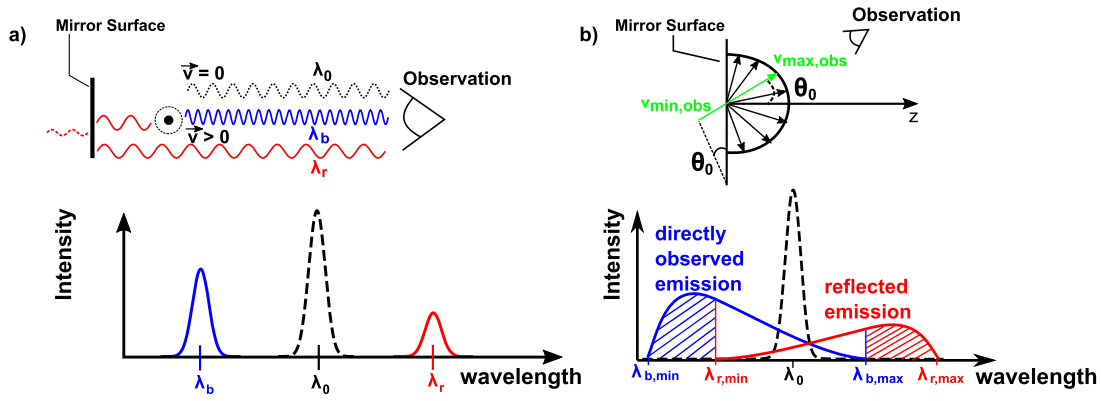

FIG. 1. (a) Schematic picture of the Doppler-shifted emission induced by an isolated and monoenergetic atom moving with the velocity v in front of the mirror toward the detector. (b) Schematic picture of the Doppler-shifted emission of the reflected atoms as a result of the plasma surface interaction. The line of sight has an angle θ_0 relative to the surface normal. The emission intervals of the blue-shifted $[\lambda_{b_{\min}}, \lambda_{b_{\max}}]$ and the red-shifted $[\lambda_{r_{\min}}, \lambda_{r_{\max}}]$ signals overlap at arbitrary θ_0, and the shape of the emission is determined by the angular and energy distribution of the reflected atoms.[7] An example of the modelled Doppler-shifted emission of the direct and reflected signals observed at the angle of 35° relative to the normal is shown in (b), bottom. For the angular distribution, a cosine distribution is assumed. For the energy distribution, the function $f(E) = (1 - x)/(2 - a - x)^b$ is used, with $a = 0.85$, $b = 2.5$, and $x = E/E_0$, where E is the energy of the reflected atoms and E_0 is the energy of the incident ions. This function approximates the TRIM calculations by Eckstein and Biersack[8] for the collision of H on W. Other analytical approximations of the TRIM code calculations can be found for instance in the work of Xia *et al.*[9] where the fitting parameters depend on the choice of the projectile-target system.

wavelength, and c is the speed of light in a vacuum. The photon emission is usually isotropic. In this case, if the emission of atoms occurs on the distances l_{λ_0} much smaller than the dimension of the mirror S ($l_{\lambda_0} \ll S \ll r$) and the latter is much less than the distance r between the observer and the mirror, then the photons reflected at the mirror will be detected at the red-shifted wavelength λ_r [Fig. 1(a), bottom]. The intensity of the red-shifted signal is reduced relative to the intensity of the blue-shifted signal by the reflectance of the mirror. The spectral reflectance at the wavelength λ_0 can be calculated by

$$R(\lambda_0) = \frac{\int I_r(\lambda) d\lambda}{\int I_b(\lambda) d\lambda}. \quad (1)$$

The profile of the blue-shifted component is in general determined by the different broadening mechanisms in the plasma such as the Doppler or Stark broadening. In the case of pure mirror-like reflectance, the whole profile of the red-shifted signal must be symmetrical to the blue-shifted one and only its amplitude is reduced.

The emission of the Balmer lines induced by fast hydrogen or deuterium atoms in the plasma represents the most suitable atomic system to realize this scheme of measurements in laboratory plasmas. Among all elements at the same energy, the Doppler-shift is the largest for hydrogen or deuterium. Extensive experimental studies of emission of atoms at the plasma surface interface in low pressure discharges and fusion plasmas demonstrated the enhanced emission of the Balmer lines in the presence of noble gases such as argon.[10–13] In fact, it was already mentioned in earlier studies[14–17] that the photons reflected at the surface could provide an additional source of emission at the red-shifted wavelengths. However, in high pressure discharges (10–100 Pa), the observed signal is a complex superposition of emission[15,18,19] induced by the incident and reflected atoms. The incident fast atoms are produced as the result of the charge-exchange recombination between the ions, being accelerated in the sheath, and the background molecules or atoms. The backscattered or reflected atoms are the result of the neutralization of the incident ions at the plasma surface. The emission of the incident atoms in the sheath enables access to the measurements of the Stark effect.[20] However, it restricts the measurement of the reflectance, according to the scheme in Fig. 1(b) considerably. In these high pressure discharges, both the directly observed emission and the reflected emission are superpositions of emission from the incident and reflected atoms. Additionally, the Stark splitting complicates the separation of lines.

In low pressure discharges, the situation is especially favorable to realize the measurements of reflectance. A recent study of the emission of fast atoms in the linear magnetized plasma, operating in the pressure range of 0.01–0.1 Pa,[21] has proven that the observed signal is induced by the reflected atoms only.[13] The following conditions are required to enable *in situ* measurements of the spectral reflectance in the plasma:

$$l_{cx} \gg d \quad (2)$$

and

$$l_{\lambda_0} \gg d. \quad (3)$$

Here $l_{cx} = 1/(n_g \sigma_{cx})$ is the mean-free path of the charge-exchange recombination of the ions in the sheath (with the neutral gas density $n_g = p/k_B T_g$, where p is the neutral gas pressure, k_B is the Boltzmann constant, T_g is the neutral gas temperature, and σ_{cx} is the charge-exchange cross section), d is the sheath thickness, and $l_{\lambda_0} = v\tau$ is the characteristic distance the atoms move before emitting a photon at the wavelength λ_0, where $\tau = 1/\sum_k A_{ik}$ is the lifetime of the excited level i and A_{ik} is the Einstein coefficient for the transition from i to k, whereas the sum extends over all lower lying levels k. Condition (2) guarantees the absence of the signal produced by the incident atoms in the sheath, impacted by the Stark effect. Condition (3) guarantees that the photons are emitted outside the sheath avoiding the impact of a strong electric field, and thus, no Stark effect on the observed line emission is expected.

In order to create fast reflected atoms in a low-density plasma, the ions need to be accelerated toward the mirror surface. To achieve this, the applied potential in the presented experiments can be varied between $U = -80$ and -220 V. At the surface, the ions are neutralized and backscattered as fast atoms.[22] They leave the surface with a certain energy and angular distribution,[7,8] as schematically shown in Fig. 1(b, top). So, for instance, for the H or D atom scattered on heavy Z materials such as W or Mo, the over-cosine angular distribution of the reflected atoms is expected.[7] The emission profile of the reflected atoms is schematically shown in Fig. 1(b) (bottom). Depending on the observation angle θ_0, the blue-shifted signal of the atoms is also partially observed at the red-shifted wavelengths and vice versa: the spectral interval of the directly observed photons is $[\lambda_0(1 - v/c), \lambda_0(1 + v/c{\cdot}\sin(\theta_0))]$, and the indirectly detected signal shown in Fig. 1(b) is observed at the spectral interval $[\lambda_0(1 - v/c{\cdot}\sin(\theta_0)), \lambda_0(1 + v/c)]$. The value of the spectral reflectance $R(\lambda_0)$ can be determined by the ratio between the non-overlapping parts of the red- and blue-shifted parts of the spectrum [compare Eq. (1)].

A demonstration that the emission of fast atoms can be applied for the spectral reflectance measurements has been shown in recent papers.[10,13] It is reported that the strongest signal of the Balmer lines generated by the reflected atoms is observed for Ar–H mixed plasmas (at flow ratios close to 1:1) where the signal depends solely on the relative kinetic energy in atom-atom collisions.[13] The kinetic energy of reflected atoms can be selectively controlled by the applied potential. In this way, the emission of fast atoms can be switched on and off as required.

The focus of this paper is to show that the signal induced by reflected atoms in low-density Ar–H plasmas can be used as an effective diagnostic tool to derive the values of spectral reflectance of metallic mirrors without additional calibration source and without removing the mirror from the plasma. Spectra were measured for a set of various mirror materials and different negative potentials.

III. EMISSION SPECTRA OF THE H_α LINE AT DIFFERENT MIRROR MATERIALS

The measurements of emission were carried out in the linear plasma device PSI-2.[21,23] The plasma is generated by a hot cathode arc discharge utilizing a hollow LaB_6 cathode. The plasma particles, created in the cathode region, move in the axial direction and are radially confined by a cylindrical magnetic field of 0.1 T generated by six magnetic field coils. The magnetic field and the geometry of the setup in the cathode-anode region reduce the extent plasma radius to $r \approx 5$ cm. Via an inlet system single gases or gas mixtures with a variable gas flow can be produced in the vacuum chamber resulting in neutral gas pressures (measured during discharge) between 0.01 and 0.1 Pa. The electron density is in the range of $n_e \sim 10^{10}$–10^{12} cm^{-3}, and typically the electron temperature is in the range of $T_e \sim 4$–10 eV.[21] The working gas flow of either 40 or 80 sccm for both H_2 and Ar gases was selected in the present experiments. Figure 2 shows the plasma profiles of electron density, electron temperature, and plasma potential for Ar–H plasma measured by using a single Langmuir probe.

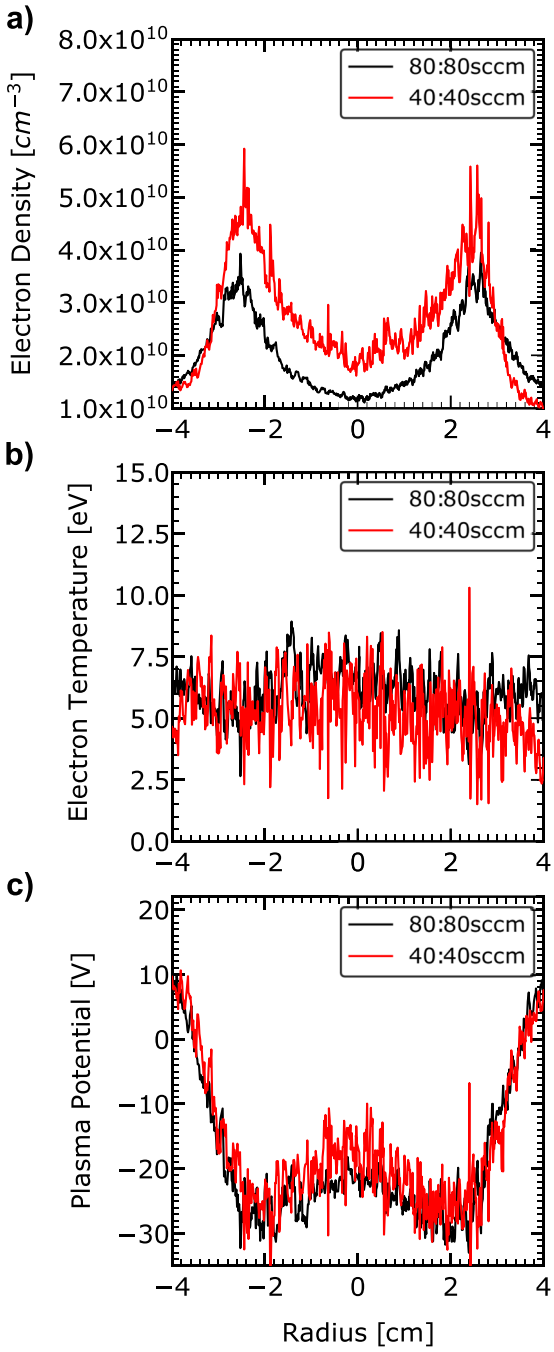

FIG. 2. Profiles of plasma parameters measured at the linear plasma of PSI-2. The results from a single Langmuir probe are shown for the Ar–H plasma at gas flow ratios of 40:40 and 80:80 sccm: electron density n_e (a), electron temperature T_e (b), and plasma potential U_p (c).

The electron density is on the order of $5{\cdot}10^{10}$ cm^{-3}, the electron temperature is about 5–7 eV, and the plasma potential is about −25 V. More detailed information about the device and its operation range can be found in Refs. 21 and 23.

The mirrors are brought into the plasma using a side manipulator at the distance of approximately 2 m downstream from the cathode. The area of the mirror is 169 mm^2 and the thickness is 2 mm. In the radial direction, the mirror is located at r ≈ 2.5 cm in the density maximum of the hollow profile, as shown in Fig. 2. The spectral emission of the fast atoms is measured at two different lines of sight, corresponding to

the angles of 35° and 90°. We note that the measurements at the angle of 90° do not provide the reflectance data since the line of sight is parallel to the mirror surface. The spectrum is measured with a high-resolution echelle spectrometer being connected with the PSI-2 device by optical fibers which are approximately 50 m long. The dispersion and resolution of the spectrometer are ∼1 pm/pixel and ∼5 pm/pixel at 6562.7 Å, respectively. The wavelength calibration is performed using a deuterium-hydrogen calibration lamp by fitting the measured H_α and D_α lines on the detector to the fine-structure resolved intensities of both lines. In all cases, the H_α line measurements are performed using a 656 nm filter in front of the spectrometer entrance slit to avoid the appearance of other orders on the detector. The integration time is 300 s for all presented spectra.

First, we show that at applied voltages U between −80 and −220 V, the experimental conditions allow us to measure the spectral reflectance of metallic mirrors according to Eqs. (2) and (3). The electron density of 5×10^{10} cm^{-3}, electron temperature of 6 eV, gas pressure of 0.1 Pa, and kinetic energy of the atoms of 100 eV are assumed here. Using the expression for the Child-Langmuir sheath[24] in the low-collisional regime, one obtains a sheath thickness of $d \approx 0.5$ mm. The mean-free path of ions can be estimated as $l_{cx} \approx 2.6$ m using the value for the charge-exchange cross section of $\sigma_{cx} = 3 \times 10^{-15}$ cm^2 (taken from the work of Janev *et al.*[25]) and a neutral gas density n_g of 1.25×10^{12} cm^{-3}, assuming a neutral gas pressure of 0.1 Pa and a neutral gas temperature of 0.5 eV. Finally, the distance the atoms move before they can emit the detectable amount of photons in the case of the H_α line l_{λ_0} is equal to 1.4 mm (assuming a hydrogen atom with an energy of 100 eV and a lifetime of excited $n = 3$ levels $\tau = 10$ ns[26]). This distance is also less than the characteristic size of the mirror of 13 mm. Thus, all the necessary conditions at the PSI-2 device are fulfilled to measure the spectral reflectance of metallic mirrors. Figure 3 shows the measured spectra along both lines of sight for different applied potentials for the Pd mirror. Taking the Doppler effect into account, the wavelength scales of the spectra are plotted as energy scales, whereas the negative energy values correspond to observed wavelengths smaller than the wavelength of the unshifted line. The spectra consist of a strong background H_α line[27] and a very weak D_α line. No emission induced by the reflected atoms could be observed at the floating potential $U = -30$ V. By increasing the absolute value of the negative potential to 80 V, the rapid rise of emission of the reflected atoms becomes visible in Figs. 3(a) and 3(b). The observed intensity increases and the line becomes broadened. The strongest intensity for both lines of sight is achieved at a negative potential between −120 and −140 V. Further increase in the absolute potential leads to the reduction in the intensity while the width of the red- and blue-shifted wings increases. In all cases of the applied negative potential, the measured spectra in (a) reproduce the scheme shown in Fig. 1(b) (bottom). The red-shifted signal behaves identically to the blue-shifted one. By contrast, the profiles are symmetrical for 90° observation [Fig. 3(b)]. Also in this case, the observed energy of the emission correlates with the applied negative potential. The steepness of the gradient of emission is also reduced. By increasing the absolute amplitude of the applied voltage to 140 V and higher, the emission

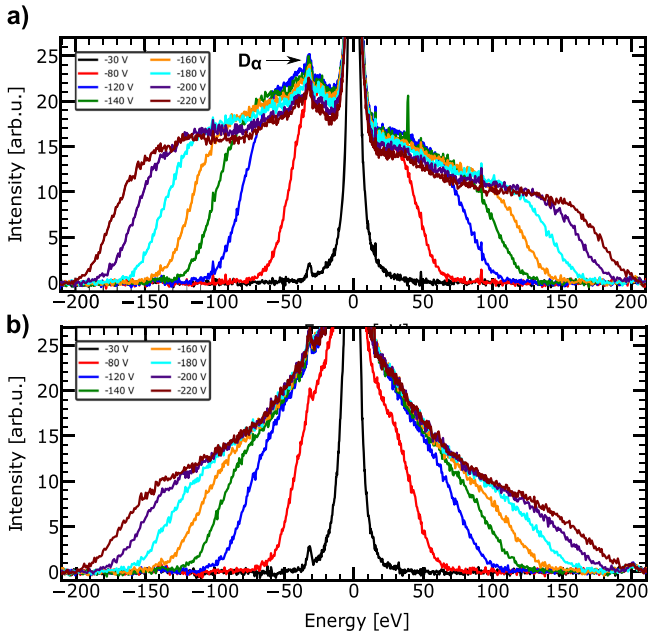

FIG. 3. Measurements of the H_α line for different applied electrostatic potentials to the Pd mirror. The spectra for the line of sight of 35° are shown in (a) and from 90° in (b). Different colors denote the different applied potentials.

induced by neutralization of H_2^+ at the surface becomes visible. This fact is especially pronounced in Fig. 3(a) as no overlap with the D_α line is observed here for the red-shifted interval. By increasing the absolute applied voltage to the values of 200 V and higher, one obviously observes the emission induced by the fast H(H_2^+) atoms in the plasma as well as by the change in the slope of the Doppler-shifted component.[18] On the one hand, we confirm the observation from high density plasma discharges,[15] but on the other hand, by adding Ar into the hydrogen plasma, we could not detect the considerable reduction in the concentration of H^+ in favor of molecular ions H_2^+ or H_3^+. However, as the calculation of the spectral reflectance from measurements is only based on the ratio between the red- and blue-shifted intervals, the source of emission is of a weak importance. In Fig. 4, the measurements for the line of sight of 35° for the Fe and C mirrors are shown. As one can see, the red-shifted part for both elements is different, but the behavior for different applied potentials is identical to the Pd mirror. The difference can be explained with the different reflectance coefficients and the different atomic masses of the materials. The atomic mass changes the energy of the backscattered atoms [according to Eq. (4)] and thus the shape of the Doppler-shifted components. The measured spectra for C, Al, Ag, Ti, and W at the applied electrostatic potential of −100 V are shown in Fig. 5. Two effects are clearly observed. First, the ratio between the red- and blue-shifted signals changes dramatically for different materials. Second, the broadening of emission clearly correlates with the atomic mass, especially for the low Z elements. Thus, for instance, for the C mirror, the red-shifted signal is very weak and the width of the emission is the lowest among all investigated materials. In the case of the Al mirror, the picture becomes quite opposite. The red-shifted signal approaches in its intensity the blue-shifted one. The wings of the emission at the blue- and red-shifted wavelengths increase

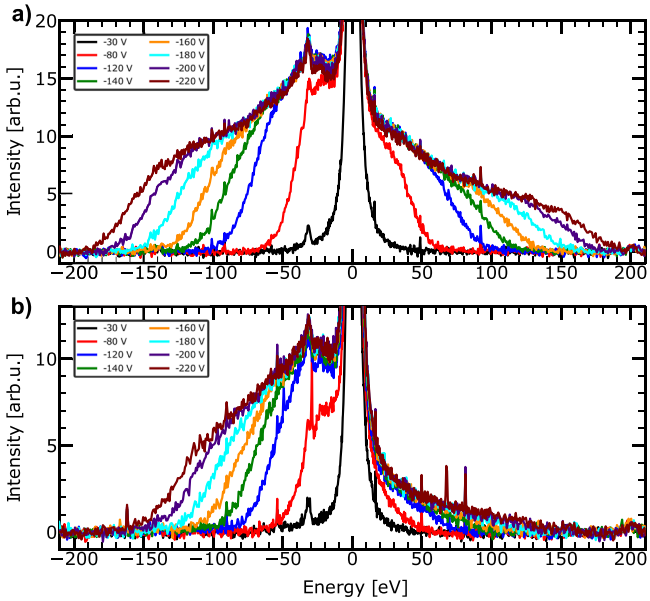

FIG. 4. Measurements of the H_α line for different electrostatic potentials. The spectra in front of the Fe and C mirrors for the line of sight of 35° are shown in (a) and (b), respectively. For both images, an Ar:H flux of 40:40 sccm is used.

too. For the Ag mirror, the profile becomes practically symmetric. For Mo, the red-shifted signal is again reduced with respect to the blue-shifted one. The increase in the red-shifted signal is observed again for the Sn mirror, and in the case of W, the red-shifted signal is nearly the half of the blue-shifted one. Whereas the measurements of reflectance depend on the ratio of the signals only, it is worth analyzing if the broadening of the emission for different materials corresponds to the general expectations. Thus, for instance, if the observed emission is caused by the reflected atoms only, then the signal is extended over the wider spectral or energy interval for higher masses of the mirror material. According to the classical formula[28] of the elastic binary collisions, the maximal kinetic energy of the reflected atoms E_m is equal to

$$\frac{E_m}{E_0} = \left[\frac{(M^2 - m^2\sin^2(\theta_0))^{1/2} - m\cos(\theta_0)}{M+m}\right]^2, \qquad (4)$$

where E_0 is the incident energy of the ions, E_m is the maximal energy of the reflected atoms, m is the mass of deuterium or hydrogen atoms, and M is the atomic mass of the mirror material. We note that Eq. (4) is expressed in the laboratory frame and the angle θ_0 is the angle between the surface normal and the line of sight. Moreover, we note that Eq. (4) is only used to calculate an upper limit of the energy because the observed emission is a result of inelastic collisions. In the low-density limit of plasma operation, the maximal kinetic energy of the incident ions is approximately equal to $E_0 \approx e(U - U_p)$, where U is the applied negative potential and U_p is the plasma potential. The measured plasma potential of the PSI-2 plasma at the position of the mirror is of −25 V, as exemplified in Fig. 2. The measured maximal energy of the reflected atoms can be estimated by calculating the onset of the H_α emission of the Doppler-shifted component E_m^p. In order to detect the

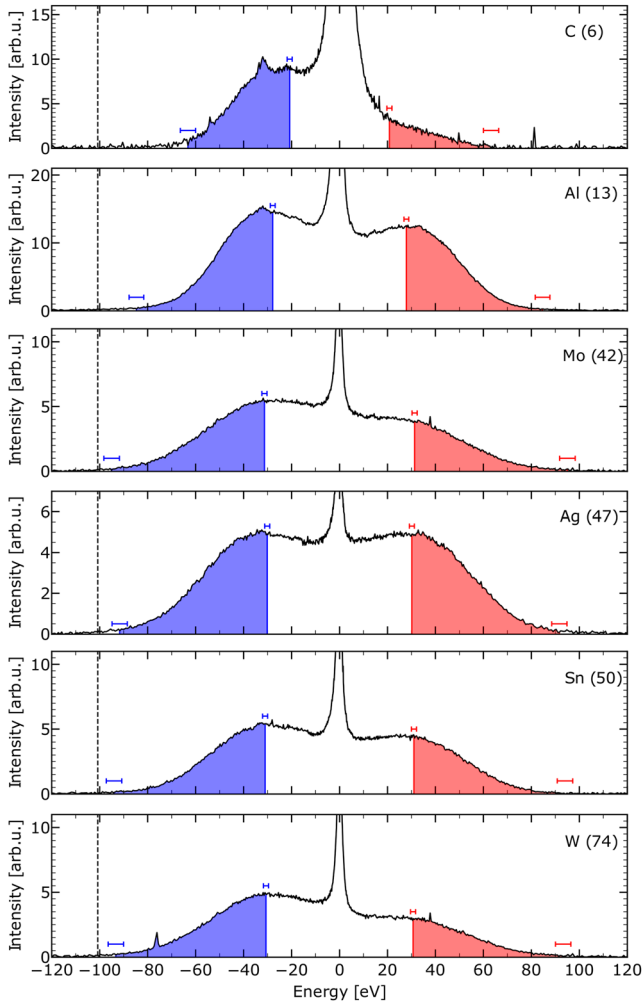

FIG. 5. Doppler-shifted emission spectra for different mirror materials (C, Al, Ag, Mo, Sn, and W) at the fixed potential of −100.8 V. The atomic number is noted in brackets. The black dashed line shows the applied potential U. The shadowed region at the red- and blue-shifted wavelength range demonstrates the overlap-free region of the direct and reflected photons. The horizontal error bars show the uncertainty in the threshold energy of the Doppler-shifted components. It results from the instrumental uncertainty which is ≈5 pixels.

boundaries of the emission signal on the level of the background, the constant background level I_b and the standard deviation σ at the blue-shifted wavelengths are calculated. Next, the wavelength and thus the energy of the emitted photons are calculated where the intensity is larger than the background value plus k times the standard deviation, i.e., $E_m^p = E(I > I_b + k \cdot \sigma)$, with k being a positive integer number. By choosing k = 3 and assuming Poisson statistics for the detected photons, one derives the onset of emission and thus the maximal energy E_m^p of the reflected atoms within 99.73% of the confidence interval. The systematic uncertainty in the spectral resolution of the spectrometer is of the order of 5 pm. This results, according to the Doppler-shift, in an uncertainty in the energy resolution of the order of 5 eV at the unshifted position of the H_α line. Note that the maximal kinetic energy of the observed photons E_m^p, derived from the Doppler-shift of the emission, must be smaller than the energy of the reflected atoms: $E_m^p = E_m - \delta E$, where $\delta E > 0$ and $\delta E \ll E_m$. δE is the part of the kinetic energy of the atoms, which is being

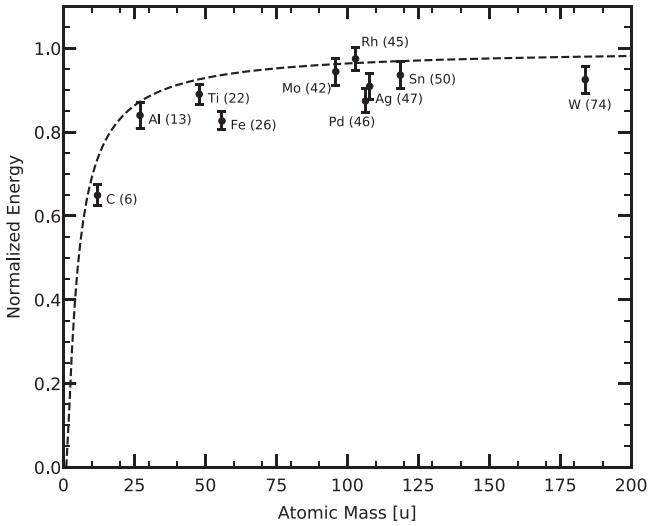

FIG. 6. Normalized energy versus the atomic mass of the different mirror materials. The experimental data for the investigated materials are shown as points. The black dashed line shows the theoretical curve calculated using Eq. (4).

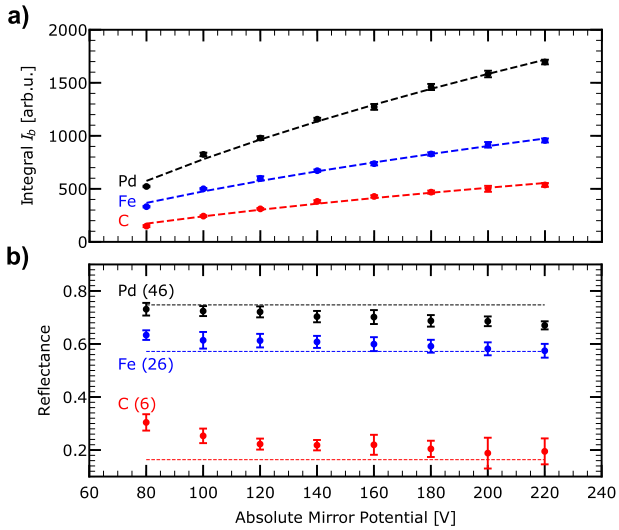

FIG. 7. Results of the spectroscopically measured reflection characteristics for the mirrors of Pd, Fe, and C. The experiments started at an applied potential of −80 V. The potential is than increased up to −220 V. (a) The integral over the blue-shifted component as a function of the applied potential. The dashed curve is a fit function $I_b = a + b\sqrt{eU}$ of the experimental data. (b) The dependence of the measured spectral reflectance on the absolute potential U. The theoretical values of reflectance are taken from the calculations of Werner *et al.*[30] for Pd and Fe and from the report of Querry[31] for C and shown as thin dashed lines.

transferred to the potential energy of the n = 3 levels of H atoms by excitation by argon atoms. Depending on the source of excitation of the fast atoms, e.g., excitation either by the ground level or by metastable levels of argon, the value $\delta E = 10.2$ eV or $\delta E = 0.12$ eV must be added to the value E_m^p to be comparable with Eq. (4). In Fig. 6, the comparison between the measured energy of the reflected atoms and the calculated one using Eq. (4) is shown. The dashed line shows the normalized energy of the atoms calculated according to Eq. (4), and the experimental energies are derived from the emission spectra of fast atoms. For the investigated materials, the measured energies E_m^p deviate not more than 10% from the calculated energies E_m. The elements with a low Z number (Z < 20) reproduce the theoretical curve well. The data points for materials with Z > 20 spread stronger, because with a greater mass the ratio E_m^p/E_m slowly reaches the value of 1 which makes it more difficult to detect the difference. Furthermore, most of the data points show a systematically lower energy compared to the calculated one: $E_m^p/E_m \approx 0.8..0.9$ as neither plasma potential nor the energy offset of 0.12 or 10.2 eV was considered in Eq. (4). The spectral reflectance of the different materials could be obtained by dividing the non-overlapping part of the reflected and direct signal of the reflected atoms in the symmetrical energy intervals of the spectra $[E_m^p \cdot \sin^2(\theta_0):E_m^p]$, as shown in Fig. 5. The corresponding integrals I_r and I_b and the errors σ_r and σ_b were calculated using the trapezoidal rule.[29] Finally, the error for the measured reflection coefficient is determined using the Gaussian error propagation formula

$$\sigma = \sqrt{\left(\frac{I_r \sigma_b}{I_b^2}\right)^2 + \left(\frac{\sigma_r}{I_b}\right)^2}. \qquad (5)$$

First, we show the results of the measurements as a function of applied negative potential for C, Fe, and Pd. Each mirror was exposed to the plasma for about 150 min. They were put under the floating potential for about 10 min, and the spectrum was recorded. Subsequently, the negative potentials of −80 V, −100 V, −120 V, −140 V, −160 V, −180 V, −200 V, and −220 V were applied. The integration time for each spectrum was 5 min, and between the measurements, the mirror remained at the last applied potential. Figure 7(a) shows the dependence of the integral I_b of the blue-shifted component on the applied electrical potential. For reflected atoms, the integral can be estimated by the following relation:

$$I_b \approx (N_+ R_N) N_{Ar,Ar^*} \langle \sigma(E_0)\sqrt{E_0} \rangle \text{ for } (U \gg U_p), \qquad (6)$$

where N_+ is the ion density of hydrogen atoms, R_N is the particle reflection coefficient for hydrogen, N_{Ar,Ar^*} is the density of argon or metastable argon,[13] and $\langle \sigma(E_0)\sqrt{E_0} \rangle$ is the rate coefficient of excitation. Following from Eq. (6), the formula $I_b = a + b\sqrt{eU}$ is used for fitting the measured integrals I_b. Figure 7(a) shows very good agreement between the measured integral and the theoretical expectation. This supports our hypothesis that the blue-shifted signal is only generated by the reflected atoms. The applied potential changes the emission rate coefficient and consequently the Doppler-shifted emission. Thus, the Doppler-shifted components can be switched on and off only by varying the applied potential. If no electrostatic potential is applied, no Doppler-shifted emission will be detectable (compare, e.g., Fig. 3).

In the case of Fe and Pd [Fig. 7(b)], the derived spectral reflectance seems to be only weakly dependent on the applied potential in the σ range and remains close to the literature values of 0.57 and 0.74[30] for all the applied potentials. A reduction in the measured reflectance is observed of the order of 5%. For C, the first value of reflectance is equal to 0.35 exceeding the literature value by more than a 50%, but for higher absolute values of applied potential, the measured ratio

approaches the literature value of 0.16.[31] This can be explained with the different kinetic energies of the atoms at different applied potentials. For the kinetic energy of the ions of 80 eV, the reflected atoms have the energy of the order of 50–60 eV. In this case, the emission of fast atoms is weak and the separation from the background component is difficult [Fig. 4(b)]. Increasing the energy of the incoming ions results in stronger emission induced by fast atoms. As a consequence, the signal-to-background ratio increases and the reflectance can be better calculated. For the mirrors of Fe and Pd, the weak variation of the measured reflectance is most probably the consequence of the weak molecular lines in the spectral region and the uncertainty of the background subtraction. In order to prove the latter fact, the Pd mirror was exposed for about 2 h in the same plasma at the applied potential of −140 V. The time dependence of the reflectance is shown in Fig. 8. Indeed within the error bars, no variation of the reflectance is detected. Also the measurements in the laboratory, before and after exposing the mirror to the plasma, indicated by the red data points only show variation of spectral reflectance of the order of 1%–2%. Apparently, the ion flow of Ar ions only weakly and slowly changes the optical properties of the mirror surface at the used plasma conditions. The comparison between the measured and the literature values of reflectance for the investigated materials is shown in Fig. 9. The data were obtained at $U = -80$ V for Fe and Pd; $U = -100$ V for Ag, W, Mo, Al, and Sn; $U = -120$ V for C; $U = -140$ V for Rh; and $U = -180$ V for Ti. The experimentally *in situ* determined reflectances are all close to the literature listed values. This fact clearly confirms that the ratio between the red- and blue-shifted signals can be used to determine the reflectance. The deviation from the literature values is at maximum ≈15%. Except for C, W, and Al, the deviation is approximately 5%. For C, the big difference can be explained with the weak red-shifted component, which makes the determination of the reflectance difficult, as explained before. For the tungsten mirror, the reflectance is larger than the theoretical value from the work of Werner *et al.*[30] This is also observed in other experiments, where the tungsten reflectance was measured. The difference between the experimental results for tungsten reflectance from the work of Minissale *et al.*[32] and ours is in the range of 7%. Thus, our results are much closer to the results of Minissale *et al.*[32] than

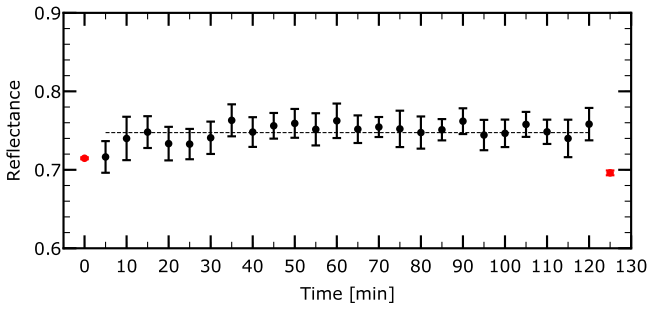

FIG. 8. Temporal evolution of the reflectance measured *in situ* for a Pd mirror. The error bars are calculated using Eq. (5). The red data points are reflectance measurements (outside the plasma using an Ulbricht sphere) before and after plasma exposure. The applied potential was $U = -140$ V, and gas flow for H_2 and Ar was 80:80 sccm. The theoretical value for Pd mirror (thin dashed line) is taken from the work of Werner *et al.*[30]

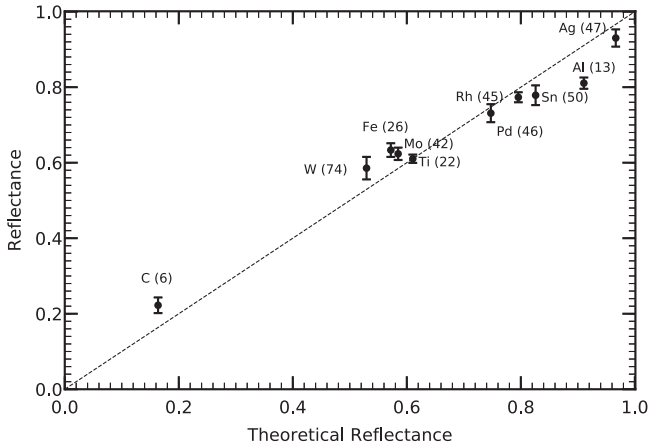

FIG. 9. Comparison between experimentally determined reflectance by using the spectroscopic method described in the present paper and the literature listed reflectance data for the materials investigated in the present work. The literature values are taken from the following references: Ag, Fe, Pd, W, Mo, and Ti (Ref. 30), C (Ref. 31), Al (Ref. 33), Rh (Ref. 34), and Sn (Ref. 35). Note that the reflectance for Sn is only known for a wavelength of 730 nm. The error bars are calculated using Eq. (5).

to the theoretical calculations of Rakić *et al.*[33] and Werner *et al.*[30]

IV. CONCLUSION AND OUTLOOK

In this paper, we presented a new spectroscopic technique, the DSRM (**D**oppler-**S**hifted **R**eflectance **M**easurement) diagnostic, which provides the possibility to measure the spectral reflectance of surfaces of electrically conductive materials in low-density Ar–H plasmas[36] without the additional use of calibration lamps or lasers. The necessary condition to measure spectral reflectance is the absence of emission due to charge exchange processes in the plasma sheath. The measurements rely only on the Doppler-shifted stimulated emission of the fast atoms reflected at the plasma-solid interface.[13] Active control of the Doppler-shifted stimulated emission is performed by varying the applied electric potential to the mirror surface. In this way, the kinetic energy of the fast reflected atoms can be controlled, and in turn, the intensity of the stimulated emission can be changed. No or very weak Doppler-shifted emission is observed for −30 V, but the emission starts to rise at applied electric potentials above −80 V. The integral over the blue-shifted emission is proportional to the square root of the kinetic energy of the ions, confirming that the signal is induced by reflected atoms only. A comparison of the measured data with the literature listed reflectance values for mirrors of several materials (C, W, Fe, Mo, Ti, Pd, Rh, Sn, Al, and Ag) shows an agreement within 15%. In spite of the obvious limitations in the precision of the measurements, e.g., the errors of order of 1%–2% in the specialized mirror laboratories could be hardly achieved using the proposed technique, the Doppler-shifted reflectance measurements can be used in low-density plasma applications where the access to the mirrors is limited.

We note, nevertheless, that the measurements were performed only for mirror-like surfaces, e.g., the analysis assumes the symmetry (except for relative intensity) between the

blue- and red-shifted profiles. However, in the case of the diffusive surfaces, the analysis probably breaks as the red-shifted emission moves toward the passive component, although the upper limit at the red-shifted wavelength is independent of the surface quality. As a result, the separation between the direct and reflected signals could be more difficult to perform.

In the forthcoming experiments, we are going to address this issue by measuring the transition from the specular to the diffusive regime and by measuring the spectral reflectance of diffusive surfaces. The polarization technique can also be applied to distinguish between the different components of the spectral reflectance for some of the materials.

ACKNOWLEDGMENTS

We thank the complete PSI-2 team for the technical and experimental support and the maintenance of the PSI-2 device.

[1]A. Litnovsky, P. Wienhold, V. Philipps, G. Sergienko, O. Schmitz, A. Kirschner, A. Kreter, S. Droste, U. Samm, P. Mertens, A. Donné, D. Rudakov, S. Allen, R. Boivin, A. McLean, P. Stangeby, W. West, C. Wong, M. Lipa, B. Schunke, G. D. Temmerman, R. Pitts, A. Costley, V. Voitsenya, K. Vukolov, P. Oelhafen, M. Rubel, and A. Romanyuk, J. Nucl. Mater. **363–365**, 1395 (2007), Plasma-surface interactions-17.
[2]S. Kajita, T. Hatae, and V. S. Voitsenya, Plasma Fusion Res. **3**, 032 (2008).
[3]M. Miyamoto, M. Yamamoto, T. Akiyama, N. Yoshida, M. Tokitani, and A. Sagara, Nucl. Mater. Energy **9**, 132 (2016).
[4]L. Moser, R. Doerner, M. Baldwin, C. Lungu, C. Porosnicu, M. Newman, A. Widdowson, E. Alves, G. Pintsuk, J. Likonen, A. Hakola, R. Steiner , L. Marot, E. Meyer, and J. Contributors, Nucl. Fusion **57**, 086019 (2017).
[5]N. Layadi, P. Roca i Cabarrocas, B. Drévillon, and I. Solomon, Phys. Rev. B **52**, 5136 (1995).
[6]F. Massines, N. Gherardi, A. Fornelli, and S. Martin, in *iCMCTF, 2005* [Surf. Coat. Technol. **200**, 1855 (2005)].
[7]W. Eckstein and J. P. Biersack, Z. Phys. A At. Nucl. **310**, 1 (1983).
[8]W. Eckstein and J. P. Biersack, Appl. Phys. A **38**, 123 (1985).
[9]Y. Xia, X. Xu, C. Tan, L. Mei, H. Yang, and X. Sun, J. Appl. Phys. **69**, 439 (1991).
[10]C. Brandt, O. Marchuk, A. Pospieszczyk, S. Brezinsek, M. Reinhart, and B. Unterberg, in 42nd EPS Conference on Plasma Physics, Lisbon, 2015, Vol. O3.J107.
[11]C. Brandt, O. Marchuk, A. Pospieszczyk, and S. Dickheuer, AIP Conf. Proc. **1811**, 130001 (2017).
[12]O. Marchuk, S. Dickheuer, C. Brandt, A. Pospiesczsyk, and A. Goriaev, "*In situ* measurements of spectral reflectivity of metallic mirrors in low density plasmas," in 44nd EPS Conference on Plasma Physics, 2017.
[13]O. Marchuk, C. Brandt, A. Pospieszczyk, M. Reinhart, S. Brezinsek, B. Unterberg, and S. Dickheuer, J. Phys. B: At., Mol. Opt. Phys. **51**, 025702 (2018).
[14]M. Adamov, B. Obradovic, M. Kuraica, and N. Konjevic, IEEE Trans. Plasma Sci. **31**, 444 (2003).
[15]M. Gemišić Adamov, M. M. Kuraica, and N. Konjević, Eur. Phys. J. D **28**, 393 (2004).
[16]T. Babkina, T. Gans, and U. Czarnetzki, Europhys. Lett. **72**, 235 (2005).
[17]N. Cvetanović, B. M. Obradović, and M. M. Kuraica, J. Appl. Phys. **109**, 013311 (2011).
[18]A. V. Phelps, J. Phys. Chem. Ref. Data **19**, 653 (1990).
[19]A. V. Phelps, Plasma Sources Sci. Technol. **20**, 043001 (2011).
[20]I. Videnović, N. Konjević, and M. Kuraica, Spectrochim. Acta, Part B **51**, 1707 (1996).
[21]A. Kreter, C. Brandt, A. Huber, S. Kraus, S. Möller, M. Reinhart, B. Schweer, G. Sergienko, and B. Unterberg, Fusion Sci. Technol. **68**, 8 (2015).
[22]P. C. Stangeby, *The Plasma Boundary of Magnetic Fusion Devices* (Institute of Physics Publishing, London, 2000).
[23]H. Kastelewicz and G. Fussmann, Contrib. Plasma Phys. **44**, 352 (2004).
[24]M. S. Benilov, Plasma Sources Sci. Technol. **18**, 014005 (2009).
[25]R. K. Janev, D. Reiter, and U. Samm, "Collision processes in low-temperature hydrogen plasmas," Berichte des Forschungszentrums Jülich, Vol. 4105, Forschungszentrum, Zentralbibliothek, Jülich, 2003, record converted from VDB: 12.11.2012.
[26]H. A. Bethe and E. E. Salpeter, *Quantum Mechanics of One- and Two-Electron Atoms* (Plenum Publishing Corporation, New York, 1977).
[27]O. Waldmann, H. Meyer, and G. Fussmann, Contrib. Plasma Phys. **47**, 691 (2007).
[28]T. L. Alford, L. C. Feldman, and J. W. Mayer, *Fundamentals of Nanoscale Film Analysis* (Springer Verlag, 2007).
[29]D. Cruz-Uribe and C. J. Neugebauer, Math. Mag. **76**, 303 (2003).
[30]W. S. M. Werner, K. Glantschnig, and C. Ambrosch-Draxl, J. Phys. Chem. Ref. Data **38**, 1013 (2009).
[31]M. R. Querry, "Optical constants of minerals and other materials from the millimeter to the ultraviolet," DTIC Report No. AD-A192 210 (1985), p. 252, available online at http://www.dtic.mil/dtic/tr/fulltext/u2/a192210.pdf.
[32]M. Minissale, C. Pardanaud, R. Bisson, and L. Gallais, J. Phys. D: Appl. Phys. **50**, 455601 (2017).
[33]A. D. Rakić, A. B. Djurišić, J. M. Elazar, and M. L. Majewski, Appl. Opt. **37**, 5271 (1998).
[34]J. H. Weaver, C. G. Olson, and D. W. Lynch, Phys. Rev. B **15**, 4115 (1977).
[35]A. I. Golovashkin and G. P. Montulevich, J. Exp. Theor. Phys. **19**, 310 (1964).
[36]O. Marchuk, C. Brandt, and A. Pospieszczyk, "Verfahren zur Bestimmung der Oberflächeneigenschaften von Targets," German patent DE102016002270B3 (10 August 2017).